

7-Chloro-5-(furan-3-yl)-3-methyl-4*H*-benzo[*e*][1,2,4]thiadiazine 1,1-Dioxide as Positive Allosteric Modulator of α -Amino-3-hydroxy-5-methyl-4-isoxazolepropionic Acid (AMPA) Receptor. The End of the Unsaturated-Inactive Paradigm?

Cinzia Citti,^{†,‡} Umberto M. Battisti,^{§,⊥} Giuseppe Cannazza,^{*,‡,§} Krzysztof Jozwiak,^{||} Natalia Stasiak,[§] Giulia Puja,[§] Federica Ravazzini,[§] Giuseppe Ciccarella,^{†,‡} Daniela Braghioli,[§] Carlo Parenti,[§] Luigino Troisi,[†] and Michele Zoli^{*,∇}

[†]Dipartimento di Scienze e Tecnologie Biologiche ed Ambientali, Università del Salento, Via per Monteroni, 73100 Lecce, Italy

[‡]CNR NANOTEC, Campus Ecotekne dell'Università del Salento, Via per Monteroni, 73100 Lecce, Italy

[§]Dipartimento di Scienze della Vita, Università di Modena e Reggio Emilia, Via Campi 103, 41125 Modena, Italy

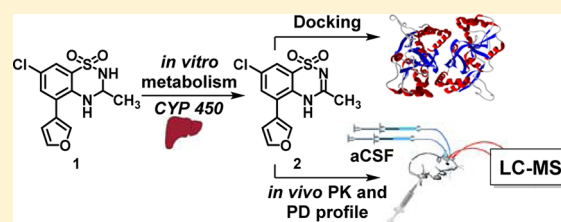
[⊥]Department of Medicinal Chemistry, School of Pharmacy, Virginia Commonwealth University, Richmond, Virginia 23298, United States

^{||}Laboratory of Biopharmacy, Department of Chemistry, Medical University of Lublin, ul. W. Chodzki 4a, 20-093 Lublin, Poland

[∇]Dipartimento di Scienze Biomediche, Metaboliche e Neuroscienze, Università di Modena e Reggio Emilia, Via Campi 287, 41125 Modena, Italy

ABSTRACT: 5-Arylbenzothiadiazine type compounds acting as positive allosteric modulators of α -amino-3-hydroxy-5-methyl-4-isoxazolepropionic acid receptor (AMPA-PAMs) have received particular attention in the past decade for their nootropic activity and lack of the excitotoxic side effects of direct agonists. Recently, our research group has published the synthesis and biological activity of 7-chloro-5-(3-furanyl)-3-methyl-3,4-dihydro-2*H*-1,2,4-benzothiadiazine 1,1-dioxide (**1**), one of the most active benzothiadiazine-derived AMPA-PAMs *in vitro* to date. However, **1** exists as two stereolabile enantiomers, which rapidly racemize in physiological conditions, and only one isomer is responsible for the pharmacological activity. In the present work, experiments carried out with rat liver microsomes show that **1** is converted by hepatic cytochrome P450 to the corresponding unsaturated derivative **2** and to the corresponding pharmacologically inactive benzenesulfonamide **3**. Surprisingly, patch-clamp experiments reveal that **2** displays an activity comparable to that of the parent compound. Molecular modeling studies were performed to rationalize these results. Furthermore, mice cerebral microdialysis studies suggest that **2** is able to cross the blood–brain barrier and increases acetylcholine and serotonin levels in the hippocampus. The experimental data disclose that the achiral hepatic metabolite **2** possesses the same pharmacological activity of its parent compound **1** but with an enhanced chemical and stereochemical stability, as well as an improved pharmacokinetic profile compared with **1**.

KEYWORDS: AMPA receptor, benzothiadiazines, hepatic metabolism, microdialysis, central nervous system, neurotransmitters



The base L-glutamate is the principal excitatory neurotransmitter ubiquitously expressed in the mammalian central nervous system (CNS), and its signal transduction is mediated by metabotropic and ionotropic receptors.^{1–3} An overstimulation of glutamate receptors observed during stroke, ischemia, and similar acute insults, mainly due to uncontrolled release of glutamate, leads to excitotoxicity. On the other hand, an insufficient stimulation of these receptors seems to be involved in learning and memory deficits associated with neurodegenerative diseases like Alzheimer's disease and schizophrenia.⁴ In the last decades, considerable effort has been devoted to the development of compounds able to enhance the glutamatergic function without causing neurotoxicity. In this context, there is a rapidly growing interest in

positive allosteric modulators of α -amino-3-hydroxy-5-methyl-4-isoxazolepropionic acid receptor (AMPA-PAMs) for their therapeutic properties as enhancers of glutamatergic transmission without the side effects associated with direct agonists.^{2–4} Several AMPA-PAMs have been described in the last two decades.^{5–13} These molecules bind to an allosteric site and enhance AMPA receptor (AMPA) activity by decreasing desensitization or deactivation.¹⁴ Among the different chemical classes of AMPA-PAMs, benzothiadiazines are one of the most investigated, due to their potential utility for a variety of clinical

Received: September 29, 2015

Accepted: November 18, 2015

Published: November 18, 2015

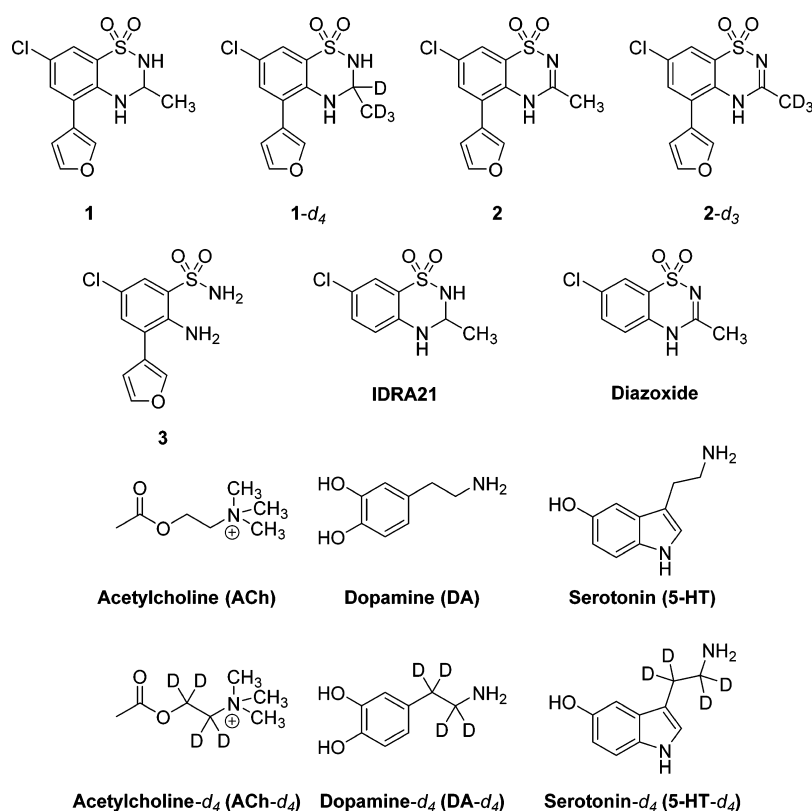


Figure 1. Structures of analytes of interest. 7-Chloro-5-(furan-3-yl)-3-methyl-3,4-dihydro-2H-benzo[*e*][1,2,4]thiadiazine 1,1-dioxide (**1**), 7-chloro-5-(furan-3-yl)-3-methyl-4H-benzo[*e*][1,2,4]thiadiazine 1,1-dioxide (**2**), and 5-chloro-3-(3-furyl)-2-aminobenzensulfonamide (**3**). Compound **2** is obtained from the hepatic degradation of **1**, differing from the latter by a C–N double bond on the thiadiazine ring. Compound **3** derives from the hydrolysis of compound **1**. Their deuterated analogues, 7-chloro-5-(furan-3-yl)-3-(methyl-*d*₃)-3,4-dihydro-2H-benzo[*e*][1,2,4]thiadiazine 1,1-dioxide-3-*d* (**1-d**₄) and 7-chloro-5-(furan-3-yl)-3-(methyl-*d*₃)-4H-benzo[*e*][1,2,4]thiadiazine 1,1-dioxide (**2-d**₃) are also shown; they were used as internal standards (ISs). IDRA21 is the lead compound for C5-substituted benzothiadiazine derivatives, and diazoxide is its corresponding unsaturated derivative. Acetylcholine (ACh), dopamine (DA), serotonin (5-HT), and their deuterated analogues, ACh-*d*₄, DA-*d*₄, and 5-HT-*d*₄ (ISs), are also shown in the figure. The changes in the levels of these neurotransmitters were investigated after intraperitoneal administration of **2** (2 mg/kg).

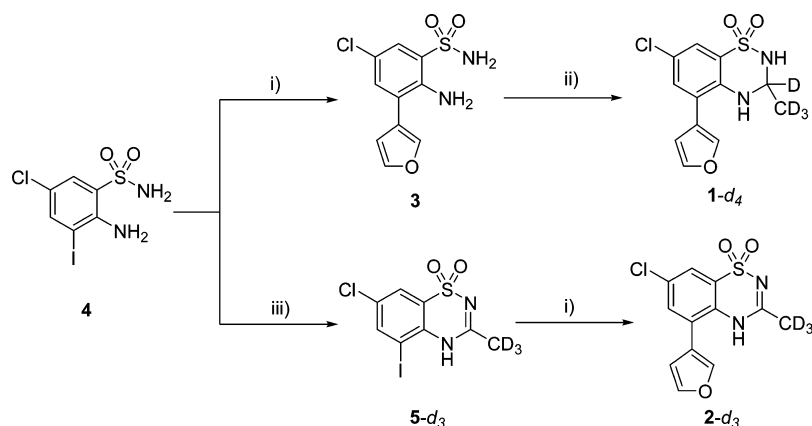
indications such as schizophrenia, depression, Alzheimer's disease, Parkinson's disease, attention deficit hyperactivity disorder (ADHD), and respiratory depression.^{12,13,15–20} Within the benzothiadiazines class, 7-chloro-5-(furan-3-yl)-3-methyl-3,4,6,7-tetrahydro-2H-benzo[*e*][1,2,4]thiadiazine 1,1-dioxide (**1**, Figure 1), recently developed by our research group, showed an interesting activity in *in vitro* tests, thus proving to be one of the most active benzothiadiazine-derived AMPA-PAMs ever reported.²¹ Moreover, cerebral microdialysis experiments indicated that **1** is able to cross the blood–brain barrier (BBB) after intraperitoneal (ip) injection since it was detected at micromolar concentration in mouse nucleus accumbens (NAc) dialysates.²¹

The notable pharmacological profile of **1** suggested that it could be taken to the next stage of development in behavioral tests on experimental animals. Nevertheless, when dealing with new drug candidates, it is crucial to investigate some other important aspects, such as the pharmacokinetic (PK) profile and *in vivo* stability of the compound under investigation. With regard to the first point, mouse cerebral microdialysis experiments showed a relatively fast time course for compound **1**, since it reached a peak in concentration 40 min after the injection, then decreased until it disappeared within the following 1.5 h.²¹ This is a fundamental feature to consider for compounds acting on the CNS, because they should remain

in the area of interest for sufficient time at the appropriate concentration to evoke the desired therapeutic effect.

Furthermore, as mentioned above, *in vivo* chemical and stereochemical stability are among the most important properties to be considered. In fact, chemical degradation of a pharmacologically active compound can lower the intended concentration below the therapeutic dose. Additionally, it has been shown that the AMPA-PAM activity resides in mainly one enantiomer.²² Thus, it is necessary to obtain the single enantiomers to perform single pharmacological tests. To this end, it is required to establish whether a drug-like molecule is stable under physiological conditions. However, recent studies suggested that, despite its stability to acidic hydrolysis, compound **1** undergoes a fast enantiomerization in aqueous media due to the lability of the C-3 stereogenic center.²³ Therefore, *in vivo* administration of a single enantiomer of **1** appears to be meaningless.

Moreover, cerebral microdialysis experiments coupled to liquid chromatography–tandem mass spectrometry with electrospray ionization (LC-ESI-MS/MS) revealed the presence of a moderate amount of 7-chloro-5-(furan-3-yl)-3-methyl-4H-benzo[*e*][1,2,4]thiadiazine 1,1-dioxide (**2**) (Figure 1) in mouse NAc after ip administration of **1**. 5-Chloro-3-(3-furyl)-2-aminobenzensulfonamide (**3**, Figure 1), formed by acid-catalyzed hydrolysis of **1**, was also detected, although only in traces. The formation of **2** is most likely due to the enzymatic

Scheme 1. Synthesis of Deuterated Internal Standards 1-*d*₄ and 2-*d*₃^a

^aReagents and conditions: (i) furan-3-ylboronic acid, Pd(PPh₃)₄, Na₂CO₃, H₂O/dioxane; (ii) deuterated acetaldehyde, HCl, *i*PrOH; (iii) deuterated acetic acid, H₂SO₄.

action of cytochrome P450 (CYP450), since it has been reported by Francotte et al. that similar compounds are converted by the latter into the corresponding unsaturated derivatives, which were found to be inactive *in vitro* as AMPA-PAMs.²⁴ It is well-known that drug metabolism can also generate toxic molecules related to possible side effects; thus the investigation of the biological activity of the possible metabolites of a drug candidate is mandatory prior to its *in vivo* evaluation. On the other hand, previous studies showed that compounds active in the CNS could elicit their pharmacological activity *in vivo* via their metabolites since the latter could have an activity higher than the parent compound itself.^{25,26}

The first goal of the present work was to study the hepatic metabolism of compound **1** by using rat liver microsomes, which is a useful tool to obtain phase I metabolites. An LC-ESI-MS/MS method was developed in order to identify and quantify the metabolites formed by the microsomal enzymes. Subsequently, the metabolites were tested for their *in vitro* AMPA-PAM activity by patch-clamp technique. Due to the surprisingly interesting results obtained from the *in vitro* tests, a computational docking simulation was employed to rationalize the biological results. Moreover, the *in vivo* PK and pharmacodynamic (PD) profiles of metabolite **2** were also investigated. This task was accomplished by employing cerebral microdialysis technique on mice coupled to a recently developed LC-ESI-MS/MS method.²⁷ This approach allowed for the simultaneous evaluation of the time course of **2** in two target areas of the CNS (hippocampus and NAc) and of the concentration of neurotransmitters, such as dopamine (DA), serotonin (5-HT), and acetylcholine (ACh), considered a direct biomarker of the brain functional activity and of the efficacy of a CNS active drug (Figure 1).

RESULTS AND DISCUSSION

Hepatic Metabolism of 7-Chloro-5-(3-furanyl)-3-methyl-3,4-dihydro-2H-1,2,4-benzothiadiazine 1,1-Dioxide (1). The study of drug metabolism was carried out using rat liver microsomes, a subcellular fraction containing major drug-metabolizing enzymes, including the CYP450 family and flavin monooxygenase. Following a simple known literature protocol,²⁸ 5 μ L of a 10 μ M solution of the test compound **1** was incubated with 432 μ L of 0.1 M phosphate buffer, pH 7.4, 50 μ L of 10 mM NADPH, and 13 μ L of rat liver

microsomes at a protein concentration of 20 mg/mL in the same phosphate buffer. The incubation at 37 °C was carried out at t_0 (stopped straight after the addition of microsomes with ice-cold methanol) and t_{60} (stopped 60 min after the addition of microsomes). When the incubation was stopped, a centrifugation step allowed the separation of the pellet with the precipitated proteins from the supernatant. The two media (at t_0 and t_{60}) were analyzed by LC-MS in total ion chromatogram mode (TIC). A major peak at the same retention time and m/z as **1** was visible in the chromatogram corresponding to the t_0 incubation medium. After incubation of **1** for 60 min at 37 °C and subsequent separation of the incubation medium, the metabolic degradation of this compound exhibited two major metabolites. These were unequivocally identified as compounds **2** and **3** by comparing the retention time, m/z , and mass fragmentation spectrum with those of authentic synthesized compounds.

An *ad hoc* LC-ESI-MS/MS method was developed in order to evaluate the concentration of **1**, **2**, and **3** in the incubation media. In order to obtain reliable quantitative results, it is necessary to employ stable deuterated internal standards (ISs) to compensate the ion enhancement or suppression of the analytes in the ESI source due to coelution of exogenous medium salts and endogenous compounds. To this aim, stable deuterated compounds **1-*d*₄** and **2-*d*₃** have been prepared (Figure 1) and fully characterized. Compound **1-*d*₄** was synthesized following the procedure described by Battisti et al.,²¹ using deuterated acetaldehyde as the deuterium source in the final step (Scheme 1). Compound **2-*d*₃** was prepared starting from 2-amino-3-iodo-5-chlorobenzene-sulfonamide (**4**) and deuterated acetic acid to give deuterated benzothiadiazine **5-*d*₃**. The latter was then reacted with furan-3-ylboronic acid in a Suzuki–Miyaura cross coupling yielding the final compound **2-*d*₃** (Scheme 1).

A pentafluorophenylpropyl stationary phase (Discovery HS-F5) was employed for the simultaneous detection of compounds **1**, **2**, and **3**. The mobile phase was composed of water with 0.1% formic acid (solvent A) and acetonitrile (solvent B) 50:50 (v/v), pumped in isocratic mode at a flow rate of 0.3 mL/min. The ESI source of the mass spectrometer triple quadrupole was set in positive mode, and the analyses were followed in multiple reaction monitoring (MRM) mode. Two transitions, one quantifier and one qualifier, were selected

for each analyte: 299 → 218 (154), 297 → 192 (164), and 273 → 192 (102) were the transitions selected for 1, 2, and 3, respectively. The transitions 303 → 222 and 300 → 195 were selected for the deuterated ISs, 1-*d*₄ and 2-*d*₃, respectively. At *t*₀, only trace amounts of compounds 2 and 3 were visible in the chromatogram, while the presence of compound 1 is predominant (Figure 2, panel a). After 60 min of incubation

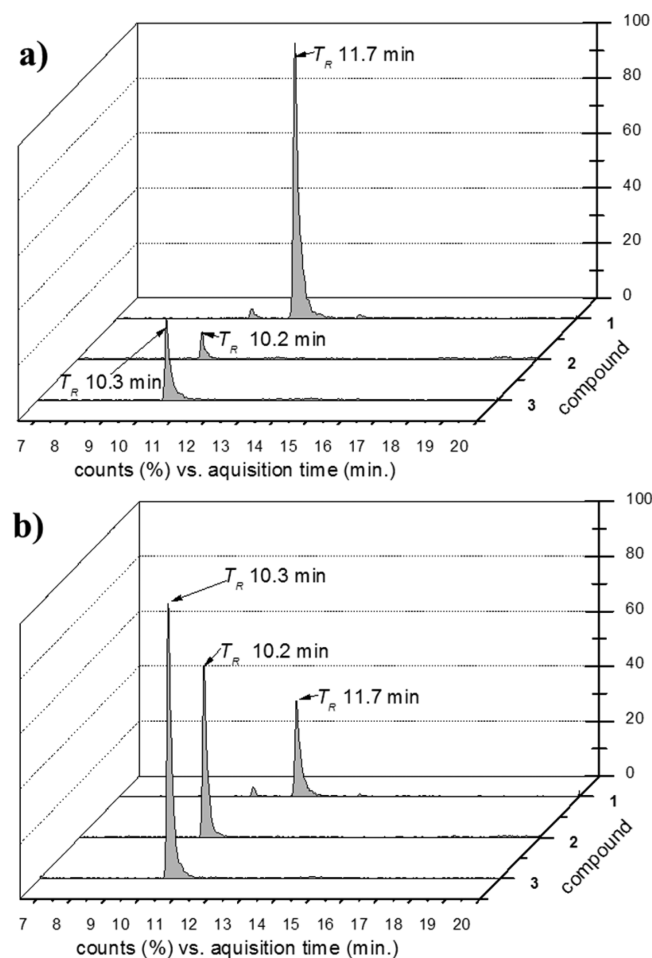


Figure 2. Chromatograms of compounds 1, 2, and 3 after incubation with rat liver microsomes at *t*₀ (panel a) and at *t*₆₀ (panel b). The retention time is indicated for each compound with an arrow connected to the corresponding peak. X axis shows the acquisition time in minutes, y axis indicates the abundance of each compound, while the chromatographic profile of the three compounds is distributed on the z axis. The graphs show a 55% decrease of the levels of compound 1 within 60 min of incubation with rat liver microsomes. The loss of the parent compound is compensated by the increase of the levels of compound 2 and, to a lesser extent, of compound 3. The concentration values were calculated using the internal standard correction.

with the microsomes (*t*₆₀), the loss of compound 1 was 60% (from 10.0 ± 0.2 to 4.0 ± 0.3 μM), and at the same time, a large increase of 2 (5.3 ± 0.2 μM) and a small increase of 3 (1.2 ± 0.1 μM) were observed (Figure 2, panel b). These experiments suggested that compound 1 is partially hydrolyzed to 3 and metabolized by the hepatic microsomes to the corresponding unsaturated metabolite 2 before reaching its target in the CNS.

In Vitro Activity of 7-Chloro-5-(furan-3-yl)-3-methyl-4H-benzo[e][1,2,4]thiadiazine 1,1-Dioxide (2) and 5-

Chloro-3-(3-furyl)-2-aminobenzensulfonamide (3). Previous studies showed that after systemic administration of 1, a moderate amount of 2 and traces of 3 were present in the CNS.²¹ Focusing our interest on these metabolites, we evaluated the activity of compounds 2 and 3 as AMPA-PAMs by patch-clamp technique using the parent compound 1 as reference. In order to compare the current activity data to compounds previously published by our group, the same methodology was selected.^{21,22,29} Compounds 1, 2, and 3 were tested at the concentration of 10 μM in primary cultures of cerebellar granule neurons. Figure 3 shows the potentiation of

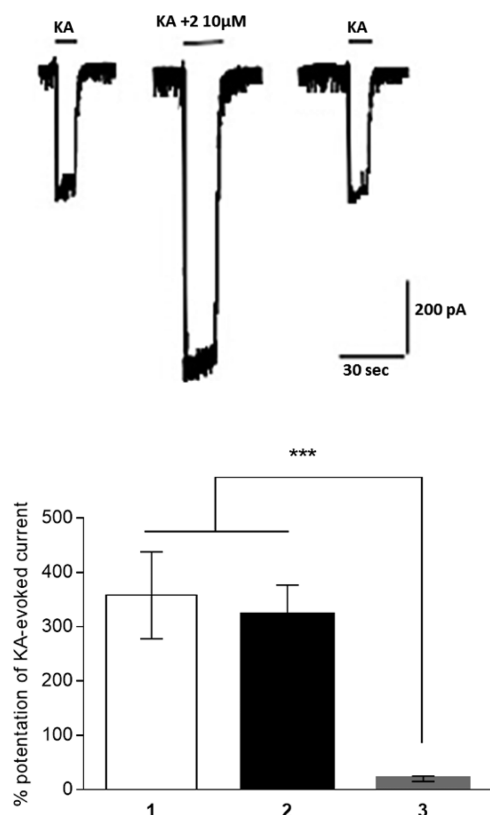


Figure 3. Upper panel: Electrophysiological traces showing the effect of compound 2 on KA (100 μM)-evoked currents recorded in primary culture of granule neurons. Lower panel: Histogram summarizing the effect (% potentiation of KA-current) of compounds 1, 2, and 3 (all at 10 μM). Each bar is the mean ± SEM of six experiments. Compound 3 shows no effect (t-test, *** means *p* < 0.001), while compounds 1 and 2 display comparable activity.

the kainate (KA)-evoked currents by the three tested compounds. The KA-evoked current was mainly mediated by AMPAR activation because application of GYKI 53655 (100 μM), an AMPA receptor antagonist, almost completely abolished the current (data not shown).²¹ Compound 3 was inactive at this concentration since no significant variations of the KA-mediated currents were observed (2% ± 5%; mean ± SEM; *n* = 6). As previously reported,²¹ compound 1 potentiated the KA-evoked currents by 358% ± 80% (mean ± SEM; *n* = 6). Pleasingly, the hepatic metabolite 2 showed a current potentiation of 323% ± 54% (mean ± SEM; *n* = 6), thus fully comparable to that of its parent compound (*t* test, *p* > 0.05). Since previous SAR studies on AMPA-PAMs revealed that the introduction of a double bond in 3,4 position of the benzothiadiazine core results in an almost 100-fold drop of

activity,^{24,30} this finding is worthy of note, suggesting that the heterocyclic substituent at C5 causes a different binding mode of the benzothiadiazine core in the receptor allosteric site. Compound **2**, possessing a suitable pharmacological profile *in vitro*, could be considered as a potential drug candidate for the potentiation of cognitive and mnemonic abilities.

Molecular Modeling. Recently, various interactions and binding modes in the receptor have been observed for benzothiadiazine type compounds active as AMPA-PAMs depending only on small structural differences.^{29,31,32} Thus, to fully understand and rationalize the unexpected biological data, docking studies were performed. Taking advantage of the crystal structures of AMPA GluA2 ligand binding domain cocrystallized with several benzothiadiazines, Molegro Virtual Docker (MVD) software was applied to dock compound **1** and its active metabolite **2** within the binding pocket of the GluA2 dimer interface. GluA2 was selected because it is the most expressed subunit in AMPAR and due to its determinant role in mammalian AMPAR function related to its calcium impermeability.^{33–35} The software MVD was previously evaluated on several crystal structures of benzothiadiazines.^{29,31} The average root-mean-square distance (RMSD) of the best ranked pose of the tested compounds compared with their binding pose in their respective crystal structures was found to be less than 1.0 Å, proving that MVD is able to accurately dock this class of compounds. The ligands were built with Spartan Wave function 08. Since compound **2** could exist as two possible tautomers (2*H*- or 4*H*-form), the difference in energy between the two tautomers was calculated (Figure 4). The 4*H*-form seems to be

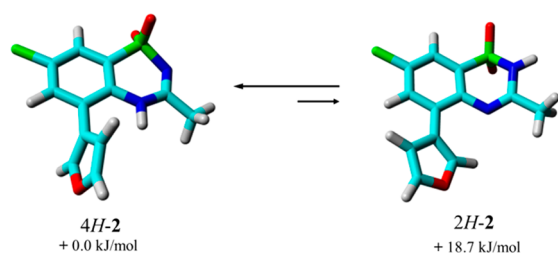


Figure 4. The two possible tautomers of **2**: 4*H*-**2** (+0.0 kJ/mol); 2*H*-**2** (+18.7 kJ/mol).

more stable than the 2*H* one with a difference in energy of 18.7 kJ/mol; therefore, according to the Boltzmann distribution, compound **2** should be predominantly in the 4*H*-form. These data are in agreement with the tautomeric conformation observed for several unsaturated benzothiadiazine in the crystalline state, which indeed is found to be the 4*H*-form.^{36–41}

Among the tested receptor crystal structures, GluA2 dimer in complex with IDRA21 (Figure 1, PDB code 3IL1) was selected for docking studies of the selected compounds due to structural similarity.³¹ The docking output clearly demonstrates that compounds **1** and **2** adopt a binding mode close to that of IDRA21 (Figure 5). The primary polar interaction partners for both compounds are Ser754 and Gly731 (Figure 6). Compounds **1** and **2** are able to form an H-bond with Ser754 with the N-4 hydrogen whereas the amidic backbone of Gly731 forms an H-bond with the oxygen of the sulfone moiety since it is located for both compounds within 4 Å. Moreover, the furanyl moiety of both compounds **1** and **2** is accommodated within the hydrophilic pocket lined by Lys763, Tyr424, Ser729, Phe495, and Ser497 residues interacting via hydrogen bond with the latter amino acid.

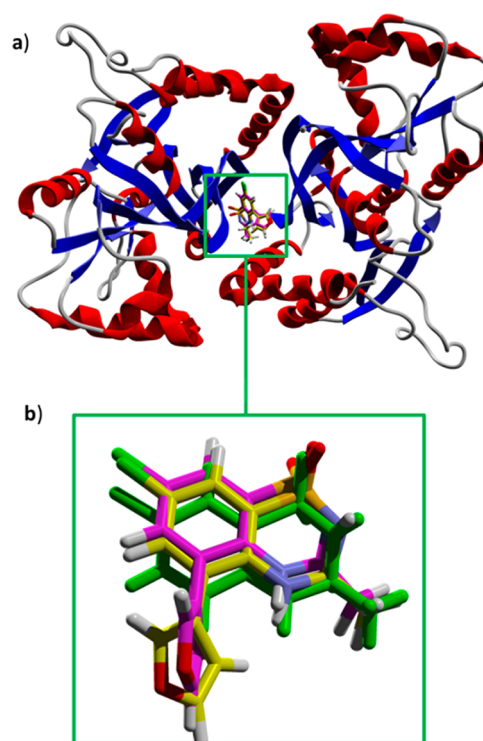


Figure 5. Compound **1** (yellow) and **2** (magenta) in GluA2 dimer interface (panel a). Binding mode of **1** (yellow), **2** (magenta), and IDRA21 (green) (panel b).

This interaction, as recently reported, is crucial in conferring high activity as an AMPA-PAM.^{21,42}

The main difference observed between **1** and **2** is the polar interaction with Pro494. In fact, the carbonyl oxygen atom of Pro494 forms a polar interaction with the N-2 atom of **1**. Differently, for compound **2** the absence of the hydrogen atom at position N-2, due to the double bond at position 2,3, prevents this interaction. The lack of this polar interaction is probably related to the slight decrease in activity observed for **2** with respect to **1**. The data obtained could also explain the great loss in activity observed for all the unsaturated benzothiadiazines with respect to their saturated analogues (e.g., diazoxide (Figure 1) vs. IDRA21).^{30,31,43,44} Ptak et al. reported that the density of diazoxide in the crystal structure of GluA2 ligand binding domain is considerably weaker than that of IDRA21, residing in a position similar to that of the hydrobenzothiadiazide ring of cyclothiazide.³¹ Probably, the lack of a supplementary interaction able to compensate for the absence of the polar interaction with Pro494 prevents an “IDRA21 based” orientation of the molecule in the ligand binding pocket leading to a great drop in activity. Differently, for compound **2** the presence of the steric interactions of the furanyl moiety and the H-bond with Ser497 are able to compensate for the lack of the polar interaction with Pro494 anchoring the molecule in an “IDRA21 based” orientation retaining the AMPA-PAM activity.

Evaluation of Hippocampal and NAc Extracellular Concentration of **1, **2**, and **3** after Systemic Administration of **2**.** Cerebral microdialysis technique is an attractive tool for the evaluation of PK profile of compounds that exert their activity on the CNS. In fact, it could provide information on the concentrations of extracellular (interstitial) concentration of free drug that reflects the actual amount available at

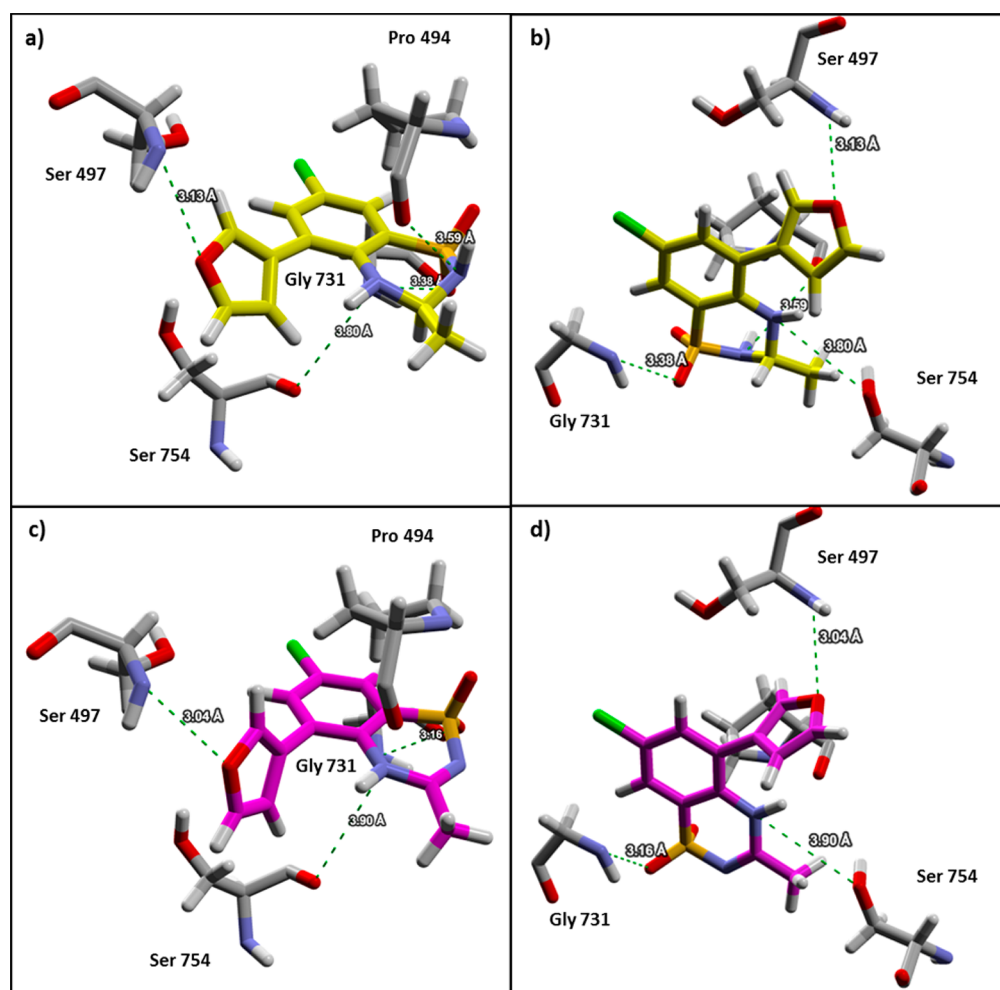


Figure 6. Principal polar interactions of **1** (yellow, panels a and b) and **2** (magenta, panels c and d). Green dashes indicate H-bond interactions.

the pharmacological target (biophase). Moreover, for pharmaceutical compounds that act on the CNS, it is essential to assess whether they are able to cross the BBB since brain PK may differ significantly from plasma PK.

Given the interesting *in vitro* activity of compound **2** as AMPA-PAM, it was necessary to evaluate its ability to reach the target in the CNS after systemic administration (2 mg/kg ip). It was previously mentioned that compound **2** was found in the brain when **1** was administered peripherally.²¹ Nonetheless, it could be argued that **1** could be metabolized by an isoform of CYP450 expressed in the cerebral tissue or on the BBB (such as CYP2D6 and CYP2B6⁴⁵). Consequently, it is possible that **2** is not able to reach the CNS due to its higher polarity compared with **1**. Therefore, it was necessary to assess its ability to cross the BBB.

In order to evaluate whether **2** can reach the CNS after systemic administration (2 mg/kg ip), cerebral microdialysis technique coupled to LC-ESI-MS/MS was employed. In particular, two microdialysis probes were inserted in the mouse hippocampus and NAc and simultaneously perfused with artificial cerebrospinal fluid (aCSF) (Figure 7).

The LC-ESI-MS/MS method previously developed was employed to determine the concentration of **2** and **3** in the dialysates. The results indicated that **2** is able to cross the BBB and reach the hippocampus and NAc within 20 min from administration without significant concentration differences in

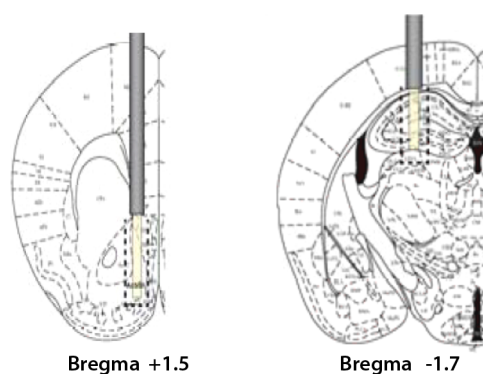


Figure 7. Schematic representation of probe location. Optimal position and range of accepted positions (dashed lines).

the two cerebral areas (*t* test, $p > 0.05$). Its concentration increased to a maximum value of about 20 nM (uncorrected for microdialysis probe recovery) after 80 min and remained constant for the next 60 min. Taking into account that the calculated microdialysis probe recovery for **2** was about 12% ($12.1\% \pm 1.7\%$), the actual concentration of the compound in the hippocampus and NAc extracellular fluid should reach about $0.17 \mu\text{M}$ 80 min after the administration of 2 mg/kg ip. Afterward its hippocampal and NAc dialysate concentrations slightly decreased to about 10 nM in the next 6 h (Figure 8).

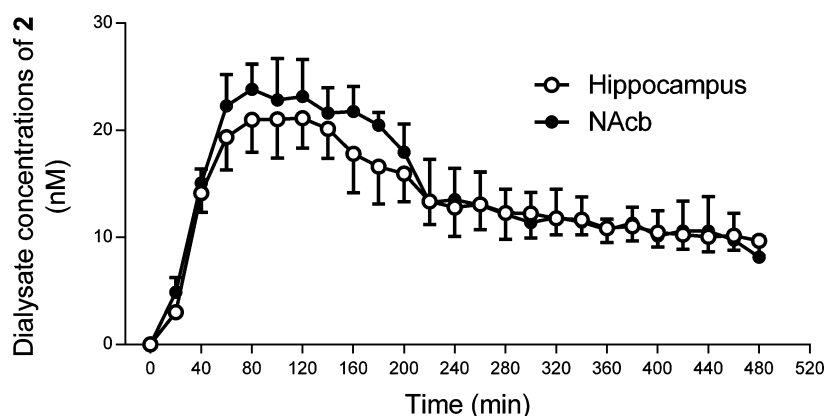


Figure 8. Time course of **2** outputs from mouse hippocampus (open circles) and nucleus accumbens (NAC, filled circles) after a single administration (2 mg/kg ip). Values are expressed in nanomolar of mean values \pm SEMs of dialysate concentrations ($n = 4$).

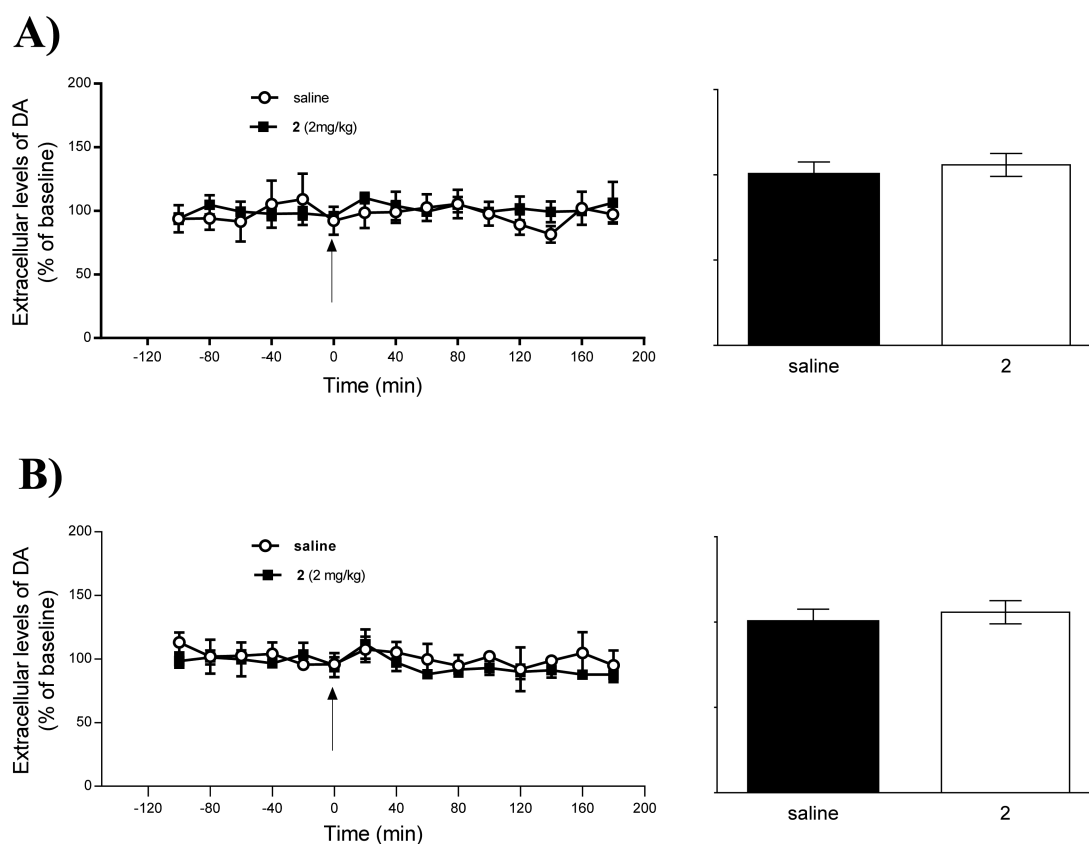


Figure 9. Microdialysis of DA extracellular levels in dorsal hippocampus (panel A) and NAc (panel B). Time course of DA extracellular levels as % of basal levels after saline and **2** injection (2 mg/kg ip). Compound **2** or saline was administered after collecting six basal samples (hippocampus basal concentration of DA 0.18 ± 0.02 nM, $n = 48$; NAc basal concentration of DA 0.57 ± 0.02 nM, $n = 48$) as indicated by the arrow. DA release is expressed as percent changes over the mean of the first six basal samples and normalized to 100%. Bars represent AUC as % of basal values for the amount of DA outflow during the first 120 min postinjection, $n = 4-5$ /group. Data plotted as mean \pm SEM.

Compounds **1** and **3** were not detected in the two cerebral areas after administration of **2** (limit of quantitation of the method, LOQ, 0.5 nM). This result indicated that **2** did not hydrolyze to the corresponding benzenesulfonamide (**3**) that could react with endogenous acetaldehyde to give **1** as previously suggested.²⁹

Interestingly, by comparing these data with our previous results,²¹ it turned out that compound **2** reaches the CNS more slowly than its parent compound and remains longer at remarkable concentrations, suggesting an increased chemical and metabolic stability with an improved PK profile.

Effects of a Systemic Administration of **2 on Hippocampal and NAc Extracellular Levels of DA, 5-HT, and ACh.** Microdialysis has gained wide recognition as an important method for *in vivo* measurement of a variety of endogenous and exogenous compounds in both blood and tissues.⁴⁶⁻⁴⁸ These include neurotransmitters and neuropeptides, enzymes, and electrolytes, as well as various hormones and pharmaceutical drugs. Measuring the changes in neurotransmitter extracellular levels in discrete brain areas can help to identify the neuronal systems involved in specific behavioral responses or cognitive processes, yielding a great deal of

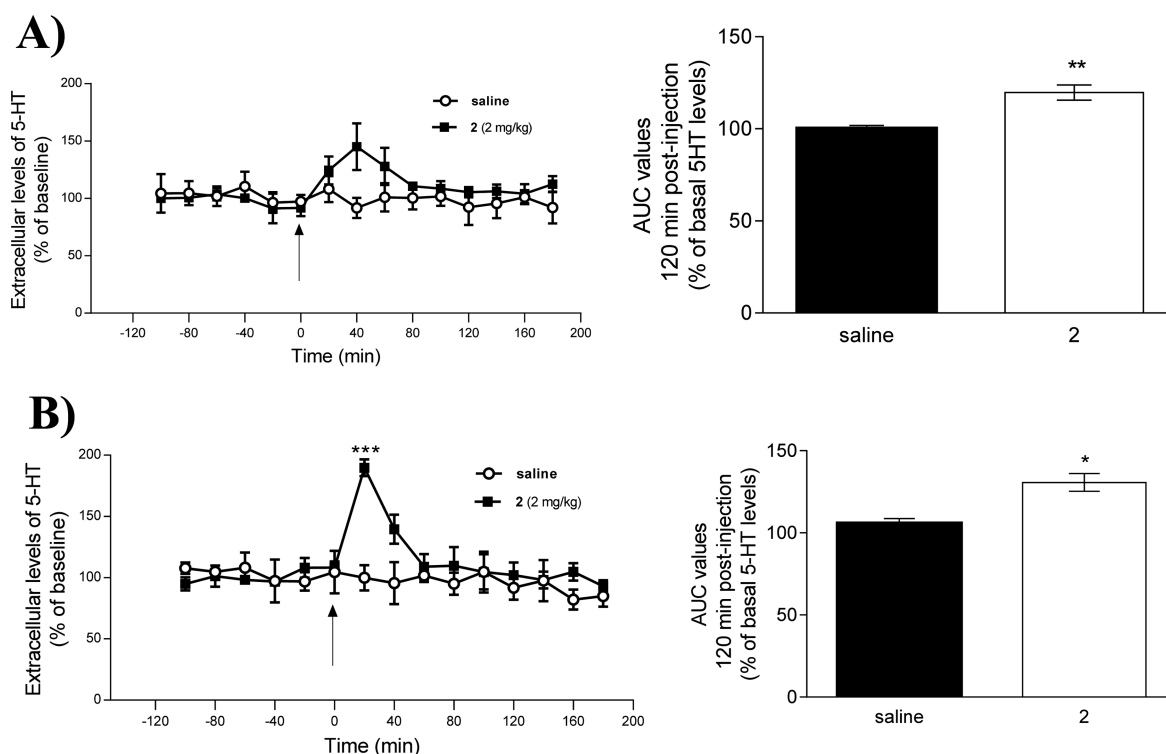


Figure 10. Microdialysis of 5-HT extracellular levels in dorsal hippocampus (panel A) and NAc (panel B). Time course of 5-HT extracellular levels as % of basal levels after saline and **2** injection (2 mg/kg ip). Compound **2** or saline was administered after collecting six basal samples (hippocampus basal concentration of 5-HT 0.13 ± 0.01 nM, $n = 48$; NAc basal concentration of 5-HT 0.14 ± 0.02 nM, $n = 48$) as indicated by the arrow. 5-HT release is expressed as percent changes over the mean of the first six basal samples and normalized to 100%. Statistical analysis was performed using one-way ANOVA and Dunnett's post-comparison test: *** $p < 0.001$ vs respective basal samples. Bars represent AUC as % of basal values for the amount of 5-HT outflow during the first 120 min postinjection, $n = 4-5$ /group. Data plotted as mean \pm SEM.

information about the functions of endogenous neurotransmitter systems.^{49,50}

We have previously showed that systemic administration of IDRA21, an AMPA-PAM structurally related to **2**, increased cerebral rat ACh levels.⁵¹ Moreover, recent unpublished results obtained by our research group suggested that compound **1** is able to increase 5-HT levels. Since several studies recently suggested that AMPA-PAMs could be effective in mood disorders, it is possible that **2** can modulate DA or 5-HT cerebral release, which are among the principal targets of therapeutics for mood disorders.⁵²

In order to evaluate whether systemic administration of **2** can influence DA, 5-HT, and ACh cerebral extracellular levels, we evaluated the dialysates concentration of neurotransmitters in mouse hippocampus and NAc by means of microdialysis.

Two microdialysis probes were inserted in mouse hippocampus and NAc, respectively, and were simultaneously perfused with aCSF. Microdialysates were directly analyzed by a recently developed LC-ESI-MS/MS method that permits the simultaneous quantification of DA, 5-HT and ACh.²⁷ Figures 9, 10, and 11 illustrate the concentrations of DA, 5-HT, and ACh, respectively, in the hippocampus (panel A) and NAc (panel B) after systemic administration of **2** (2 mg/kg ip).

DA did not show any significant changes from the basal dialysate levels in both the hippocampus and NAc (Figure 9, top and bottom, left). Moreover, the difference between DA levels in saline- and **2**-treated mice, calculated as mean AUC % between 0 and 120 min post-treatment, was not statistically significant (t test, $p > 0.05$) for both hippocampus and NAc (Figure 9, top and bottom, right).

Hippocampal 5-HT dialysate concentration increased by about 140% 40 min after the administration of **2**, although not statistically significant compared with basal levels, and slowly went back to the basal levels (Figure 10, panel A, top left). In contrast, the difference between 5-HT levels in saline- and **2**-treated mice, calculated as mean percent AUC between 0 and 120 min post-treatment, was statistically significant (t test, $p < 0.01$) (Figure 10, panel A, top right). NAc 5-HT concentration showed a peak that reached about 200% of the basal levels 20 min after the injection ($p < 0.001$), then rapidly returned to the basal levels within the next 20 min (Figure 10, panel B, bottom left). Additionally, the difference between 5-HT levels in saline- and **2**-treated mice, calculated as mean percent AUC between 0 and 120 min post-treatment, was statistically significant (t test, $p < 0.05$) (Figure 10, panel B, bottom right).

The administration of **2** elicited an increase in hippocampal ACh release, which reached a peak of about 200% 80 min after administration, then rapidly returned to the basal levels (Figure 11, panel A, top left). Furthermore, the difference between ACh levels in saline- and **2**-treated mice in the first 2 h post-treatment was statistically significant (t test, $p < 0.001$) (Figure 11, panel A, top right). Administration of **2** elicited a significant increase of NAc ACh levels in the first 20 min. Afterward the levels rapidly decreased to slightly under the basal levels (Figure 11, panel B, bottom left). No significant difference was observed between ACh levels in saline- and **2**-treated mice in the first 2 h post-treatment (Figure 11, panel B, bottom right).

These results indicate that compound **2** increases 5-HT and ACh release but not DA release both in the hippocampus and NAc. The increase of 5-HT levels could explain the effects on

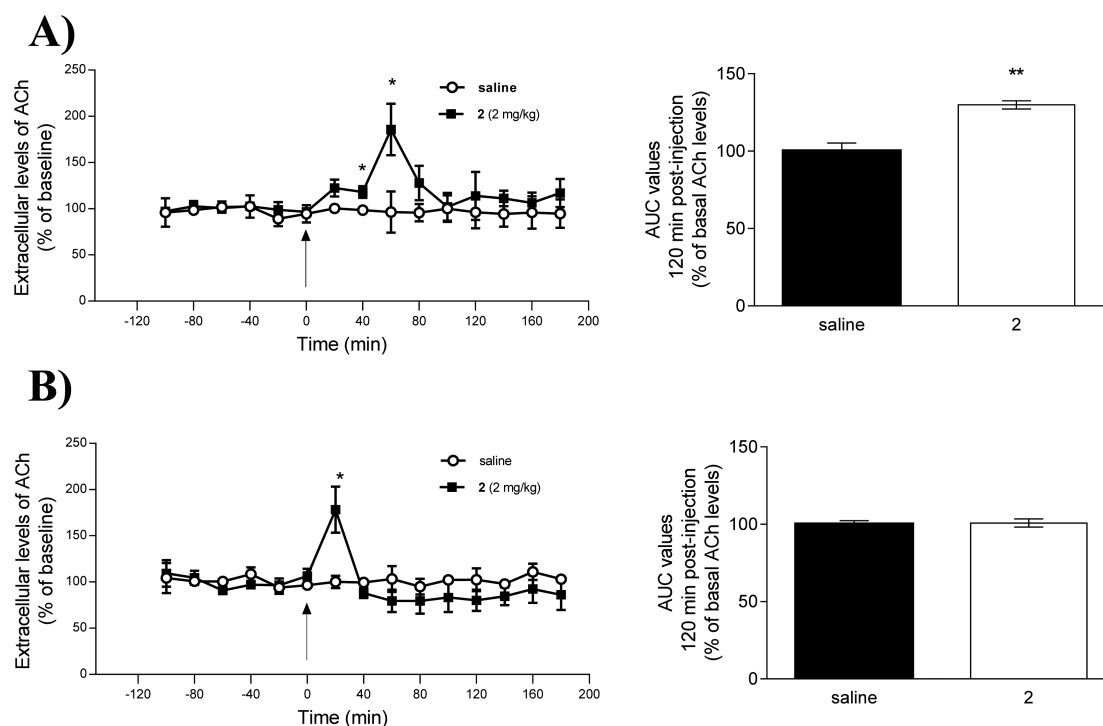


Figure 11. Microdialysis of dorsal ACh extracellular levels in hippocampus (panel A) and NAc (panel B). Time course of ACh extracellular levels as % of basal levels after saline and 2 injection (2 mg/kg ip). Compound 2 or saline was administered after collecting six basal samples (hippocampus basal concentration of ACh 0.22 ± 0.021 nM, $n = 48$; NAc basal concentration of ACh 0.24 ± 0.01 nM, $n = 48$) as indicated by the arrow. ACh release is expressed as percent changes over the mean of the first six basal samples and normalized to 100%. Statistical analysis was performed using one-way ANOVA and Dunnett's post comparison test: * $p < 0.05$ vs respective basal samples. Bars represent AUC as % of basal values for the amount of ACh outflow during the first 120 min postinjection, $n = 4-5$ /group. Statistical analysis was performed using unpaired Student's t tests: ** $p < 0.01$ vs saline. Data plotted as mean \pm SEM.

mood and motivation exerted by AMPA-PAMs.⁵² Furthermore, the increase of ACh release confirms previous results obtained by our and other research groups that suggested that the nootropic activity of AMPA-PAMs might be due not only to a potentiation of the glutamatergic transmission but also to an increase of the cholinergic one.^{51,53}

CONCLUSIONS

Our results suggest that compound 2, derived from the hepatic metabolism of 1, possesses an interesting pharmacological profile since, for the first time, it has been shown that an unsaturated benzothiadiazine derived AMPA-PAM has *in vitro* biological activity similar to that of its saturated analogue. In our opinion, compound 2 could represent a ploy to overcome the limitations associated with its parent compound. What is more, it displays advantageous chemical properties, because it should be more stable than saturated benzothiadiazine type compounds toward chemical degradation that can occur *in vivo* in the different chemical environments. Similarly, it should possess an enhanced PK profile compared with its parent compound since it is already a product of hepatic metabolism. Additionally, it does not possess stereogenic centers. Therefore, it does not entail the problems encountered with chiral drug candidates concerning the potentially different pharmacological activity of the enantiomers. Lastly, we have also demonstrated that 2 is able to increase 5-HT release in mice hippocampus and NAc, suggesting that AMPA-PAMs could also affect mood and motivation. In the same way, ACh levels increased after administration of 2, pointing out that AMPA-PAMs could exert

their nootropic activity also via the potentiation of the cholinergic transmission.

MATERIALS AND METHODS

Chemicals and Reagents. All chemicals and reagents, except those specifically noted, were purchased from Sigma-Aldrich. LC/MS grade water and acetonitrile (ACN) were purchased from Sigma-Aldrich.

Chemistry. Compounds 1, 2, and 3 were synthesized as previously described.²¹

2-Amino-5-chloro-3-iodobenzenesulfonamide (4). 2-Amino-5-chloro-3-iodobenzenesulfonamide 4 was synthesized as previously described by Battisti et al.²¹

7-Chloro-5-(furan-3-yl)-3-(methyl- d_3)-3,4-dihydro-2H-benzo[e][1,2,4]thiadiazine 1,1-Dioxide-3- d (1- d_4). To a stirring solution of 5-chloro-3-aryl-2-aminobenzenesulfonamide, 3 (100 mg, 0.37 mmol), in *i*PrOH (7 mL), acetaldehyde- d_4 (82.6 μ L, 1.47 mmol) and EtOAc saturated with HCl (3–4 drops) were added. The reaction solution was heated at 65 °C for 2 h. Subsequently water was added, and the mixture was extracted with EtOAc (3 \times 10 mL). The combined organic layers were washed with brine and dried over anhydrous Na_2SO_4 . The solvent was removed under reduce pressure to give the pure compound 1- d_4 (72%, 80 mg). ¹H NMR (CDCl_3 , 400 MHz): $\delta = 4.40$ (br s, 1H), 4.67 (br s, 1H), 6.54 (dd, $J = 0.8, 1.9$ Hz, 1H), 7.26 (s, 1H), 7.58–7.62 (m, 3H). ¹³C NMR (CDCl_3 , 100 MHz): $\delta = 19.9$ –20.4 (m), 62.1 (t), 110.3, 120.6, 121.7, 123.4, 123.5, 123.6, 133.5, 138.8, 140.6, 144.4. Mp: 150–152 °C from hexane. GC-MS (70 eV): m/z 302 (100) [M^+], 284 (54), 192 (96), 163 (52), 128 (67), 101 (31). HRMS-ESI: calculated for $\text{C}_{12}\text{H}_8\text{D}_4\text{ClN}_2\text{O}_2\text{S}$ [$\text{M} + \text{H}$]⁺ 303.0503, found 303.0509.

7-Chloro-5-iodo-3-(methyl- d_3)-4H-benzo[e][1,2,4]thiadiazine 1,1-Dioxide (5). 5-Chloro-3-iodo-2-aminobenzenesulfonamide, 4 (332 mg, 1.00 mmol), was dissolved in 15 mL of acetic acid, and subsequently

3–4 drops of sulfuric acid were added to the reaction mixture. The solution was heated to reflux during 3 h. After cooling to room temperature, the pure compound **5** was collected by filtration, washed with diethyl ether, and dried to obtain the pure compound (99%, 352 mg). ¹H NMR (DMSO-*d*₆, 400 MHz): δ = 7.90 (d, *J* = 2.2 Hz, 1H), 8.32 (d, *J* = 2.2 Hz, 1H), 10.43 (s, broad, 1H). ¹³C NMR (DMSO-*d*₆, 100 MHz): δ = 29.0, 87.9, 122.6, 122.9, 130.4, 134.9, 142.7, 159.4. Mp: melts with decomposition. FT-IR (KBr): 3321, 1569, 1466, 1376, 1299, 1162, 872 cm⁻¹. GC-MS (70 eV): *m/z* 359 (29) [M⁺], 315 (100), 251 (58), 124 (36), 97 (30). HRMS-ESI: calculated for C₈H₅D₃ClIN₂O₂S [M + H]⁺ 359.9144, found 359.9141.

7-Chloro-5-(furan-3-yl)-3-(methyl-*d*₃)-4H-benzo[*e*][1,2,4]-thiadiazine 1,1-Dioxide (2-*d*₃). To a stirring solution of 7-chloro-5-iodo-3-(methyl-*d*₃)-4H-benzo[*e*][1,2,4]thiadiazine 1,1-dioxide (352 mg, 0.99 mmol) in water/dioxane (15 mL, 1:1, v/v) Na₂CO₃ (1.05 g, 9.9 mmol), tetrakis triphenylphosphine palladium (57.8 mg, 0.05 mmol), and a 3-furanylboronic acid (133 mg, 1.19 mmol) were added. The reaction mixture was heated at 110 °C for 3 h, then allowed to gradually reach the room temperature. The mixture was neutralized with 1 M HCl solution and extracted with EtOAc (3 × 15 mL). The combined organic layers were washed with brine and dried over Na₂SO₄. The solvent was removed under vacuum, and the crude material was purified by column chromatography eluting 35% EtOAc/hexane to yield the pure compound (99%, 293 mg). *R*_f (35% EtOAc/hexane) 0.33. ¹H NMR (DMSO-*d*₆, 400 MHz): δ = 6.90 (s, 1H), 7.70 (d, *J* = 2.4, 1H), 7.81 (s, 1H), 7.90 (s, 1H), 8.18 (s, 1H), 10.69 (br s, 1H). ¹³C NMR (DMSO-*d*₆, 100 MHz): δ = 29.0, 111.1, 118.9, 121.6, 123.1, 124.6, 129.5, 131.4, 133.2, 142.5, 144.3, 158.7. Mp: melts with decomposition. FT-IR (KBr): 3297, 2358, 1603, 1496, 1289, 1158, 870. GC-MS (70 eV): *m/z* 299 (50) [M⁺], 255 (60), 191 (45), 163 (80), 128 (100). HRMS-ESI: calculated for C₁₂H₆D₃ClN₂O₂S [M + H]⁺ 300.0283; found: 300.0280.

Metabolic Studies. The experiments were performed at *t*₀ (the reaction is stopped straight after the addition of microsomes) and *t*₆₀ (the reaction is stopped 60 min after the addition of microsomes) following a known literature procedure.²⁸ The experiments were carried out using the test compound and a negative control (without NADPH). Each experiment at *t*₀ and *t*₆₀ except for the negative control was performed in duplicate. Each eppendorf tube contained 432 μL of 0.1 M phosphate buffer, pH 7.4, prewarmed at 37 °C, 50 μL of 10 mM NADPH (in the negative control it is replaced with phosphate buffer), 5 μL of test compound (10 μM solution in phosphate buffer), and 13 μL of microsomes at a protein concentration of 20 mg/mL. Each eppendorf was charged with phosphate buffer, NADPH, and test compound. They were incubated for 5 min at 37 °C. During this time, the microsomes were thawed, and then they were added to all the samples. The reactions at *t*₀ were stopped with 250 μL of ice-cold methanol, and then the mixture was well vortexed. The reactions at *t*₆₀ were incubated at 37 °C for 60 min and then stopped with 250 μL of ice-cold methanol and well vortexed. The samples were centrifuged at 10000g for 5 min at 4 °C. The supernatants were placed in HPLC vials and analyzed with the suitable LC-MS/MS method. The pellets were stored in the freezer until all the samples were analyzed.

Electrophysiological Tests. Primary cultures of cerebellar granule neurons were prepared from 7 day old Sprague–Dawley rats as reported in the literature.⁵⁴ Briefly, cells from the cerebellum were dispersed with trypsin (0.24 mg/mL; Sigma-Aldrich, Milan, Italy) and plated at a density of 0.8 × 10⁶ cells/mL on 35 mm Falcon dishes coated with poly(L-lysine) (10 μg/mL, Sigma-Aldrich). Cells were plated in basal Eagle's medium (BME; Celbio, Milan, Italy), supplemented with 10% fetal bovine serum (Celbio), 2 mM glutamine, 25 mM KCl, and 100 μg/mL gentamycin (Sigma-Aldrich) and maintained at 37 °C in 5% CO₂. After 24 h *in vitro*, the medium was replaced with a 1:1 mixture of BME and neurobasal medium (Celbio, Milan) containing 2% B27 supplement, 1% antibiotic, and 0.25% glutamine (Invitrogen). At 5 days *in vitro* (DIV5), cytosine arabinofuranoside (Ara-C) was added at a final concentration of 1 μM. Recordings were performed at room temperature under voltage-clamp in the whole-cell configuration of the patch-clamp technique on cells. Electrodes pulled from borosilicate glass (Hidellberg, FRG) on a

vertical puller (PB-7, Narishige) and had a resistance of 5–6 MΩ. Currents were amplified with an Axopatch 1D amplifier (Axon Instruments, Foster). The recording chamber was continuously perfused at 5 mL/min with an artificial extracellular solution composed of the following (mM): 145 NaCl, 5 KCl, 1 CaCl₂, 5 Hepes, 5 glucose, 20 sucrose, pH 7.4 with NaOH. Electrode intracellular solution contained the following (mM): 140 KCl, 3 MgCl₂, 5 EGTA, 5 Hepes, 2 ATP-Na, pH 7.3 with KOH. Drugs were applied directly by gravity through a Y-tube perfusion system.

Docking Studies. The GluA2-S1S2J crystal structures in complex with IDRA21 was retrieved from the Protein Data Bank (PDB code 3IL1) and imported into MVD.³¹ All water molecules and cofactors were deleted. The compounds were built in SPARTAN 08 (Wave function Inc., 18401 Von Karman Avenue, Suite 370 Irvine, CA 92612) running on a PC equipped with Intel Pentium 4 CPU, 3.40 GHz, 2 GB of RAM and Windows XP Professional. Structures generated were further optimized by Hartree–Fock *ab initio* method with 6-31G* basis set. Subsequently, they were exported as mol2 files and docked in GluA2 using MVD. We used the docking template available in MVD and evaluated MolDock score, Rerank score, and protein–ligand interaction score from MolDock and MolDock [GRID] options. IDRA21 was selected as reference compound for the template. The default settings were used, including a grid resolution of 0.30 Å and the MolDock optimizer as a search algorithm, and the number of runs was set to 10. A population size of 50, maximum iteration of 2000, scaling factor of 0.50, and crossover rate of 0.90 were used. The maximum number of poses to generate was increased to 10 from a default value of 5.

Stereotaxic Procedure and Microdialysis. Mice were anesthetized with isoflurane and placed in a flat skull position in a Kopf stereotaxic apparatus fitted with a mouse adaptor. Two guide cannulae (CMA 7, CMA Microdialysis, Stockholm, Sweden) were inserted: one into the right ventral striatum (coordinates from Bregma (in mm): anterior = +1.5, lateral = -0.5, ventral = -5.2) and one into the dorsal hippocampus (coordinates from Bregma (in mm): anterior = +1.6, lateral = ±1.3, ventral = -1.6). The guide cannulae were permanently secured with epoxy glue. After surgery, the mice were placed in a Plexiglas cage and allowed to recover overnight. After surgery (24 h), the awake animal was gently restrained by the experimenter, and a microdialysis probe (CMA 7/2, 2 mm dialysis membrane, CMA Microdialysis, Stockholm, Sweden) was inserted into each guide cannula. The probes were connected to a microinjection pump (CMA/100, CMA Microdialysis, Stockholm, Sweden) and perfused with artificial cerebrospinal fluid (aCSF, KCl 2.5 mM, NaCl 125 mM, CaCl₂ 1.26 mM, MgCl₂ 1.18 mM, Na₂HPO₄ 2 mM, pH 7.4) at a flow rate of 1.1 μL/min. Starting 1 h after implantation, dialysate samples were collected every 20 min into glass vials containing 5 μL of antioxidant solution (EDTA 0.27 mM, L-cysteine 3.3 mM, ascorbic acid 0.5 mM, acetic acid 0.1 M; 27 μL/20 min sample). Three hours after probe insertion, animals received an injection of compound **2** (2 mg/kg, ip, free base) or saline. At the end of each experiment, the animal was killed by rapid decapitation, its brain was removed from the skull, and the position of the microdialysis probes was verified by visual inspection of the fresh tissue. The probe track was visible as a small hemorrhagic line. Data from brains with large hemorrhages (more than 1 mm in diameter) were discarded. The implantation site was identified according to the mouse brain atlas.⁵⁵ All procedures were carried out in accordance with European Commission directives 219/1990 and 220/1990 and approved by Ethical commission of the University of Modena and Reggio Emilia.

LC-ESI-MS/MS for Determination of 1, 2, and 3 in Microsomal Incubation Medium and Microdialysates. Discovery HS-F5 was the column employed for the simultaneous detection of (±)-**1**, compound **2**, and the hydrolysis product **3**; the mobile phase was composed of water with 0.1% formic acid (solvent A) and acetonitrile (solvent B) 50:50 (v/v), pumped in isocratic mode at a flow rate of 0.3 mL/min. An Agilent 6410 triple quadrupole-mass spectrometer with an electrospray ion source operating in positive mode was used to analyze the microsomal extracts and mouse cerebral microdialysates. The analyses were followed in MRM mode to improve the sensitivity:

299 → 218 (154), 297 → 192 (164), 273 → 192 (102), 303 → 192, and 300 → 218 were the transitions selected for 1, 2, 3, 1-*d*₄, and 2-*d*₃, respectively. 1-*d*₄ and 2-*d*₃ were used as the internal standards. The chromatograms were integrated using Agilent Mass Hunter software.

LC-ESI-MS/MS for Determination of DA, 5-HT, and ACh. For ACh, DA, and 5-HT detection, a 20 μ L volume from each sample was injected into an Agilent 6410 triple quadrupole-mass spectrometer with an electrospray ion source operating in positive mode as previously described by Cannazza et al.²⁷ Discovery HS-F5 column (150 mm \times 2.1 mm, 3 μ m; Sigma-Aldrich, Milan, Italy) was used for chromatographic separations. The mobile phase was composed of water with 0.1% formic acid (solvent A) and acetonitrile (solvent B). HPLC analyses were carried out using an elution profile composed of a first isocratic step of 5% of B for 1.5 min and then to 30% of B over 6 min at 25 °C. The column was washed with 90% of B for 2.5 min followed by the equilibration of the column for 5 min with 5% of B. The flow rate was 0.3 mL/min. As set for 1, 2, and 3, the following transitions were selected: 158 → 141 (91), 177 → 160 (115), and 146 → 87 (60) for DA, 5-HT and ACh, respectively. DA-*d*₄, 5-HT-*d*₄, and ACh-*d*₄ were used as internal standards and 162 → 141, 181 → 160, and 150 → 87, respectively, were the corresponding transitions.²⁷

AUTHOR INFORMATION

Corresponding Authors

*Tel: +39 059 2055013. Fax +39 059 2055750. E-mail address: giuseppe.cannazza@unimore.it (Giuseppe Cannazza).

*Tel: +39 059 2056511. Fax: +39 059 245156. E-mail address: michele.zoli@unimore.it (Michele Zoli).

Author Contributions

M. Zoli and G. Cannazza were responsible for the supervision and development of the whole project. C. Citti carried out the metabolic studies. G. Cannazza and N. Stasiak performed the microdialysis experiments. U. M. Battisti and K. Jozwiak performed the molecular modeling studies. G. Puja and F. Ravazzini conducted the electrophysiological tests. C. Citti, G. Cannazza, and G. Ciccarella performed the LC-MS/MS analyses. D. Braghiroli, C. Parenti, and L. Troisi were responsible for the chemical synthesis of the molecules presented in this paper.

Notes

The authors declare no competing financial interest.

ABBREVIATIONS

ACh, acetylcholine; ADHD, attention deficit hyperactivity disorder; AMPA, α -amino-3-hydroxy-5-methyl-4-isoxazolepropionic acid; AMPA-PAM, positive allosteric modulator of AMPA receptor; AMPAR, AMPA receptor; BBB, blood–brain barrier; CNS, central nervous system; CYP450, cytochrome P450; DA, dopamine; EGTA, ethylene glycol tetraacetic acid; Hepes, 4-(2-hydroxyethyl)-1-piperazineethanesulfonic acid; 5-HT, serotonin; ip, intraperitoneal; IS, internal standard; KA, kainic acid; kyn, kynurenine; LOQ, limit of quantitation; MRM, multiple reaction monitoring; MVD, Molegro Virtual Docker; NAc, nucleus accumbens; PD, pharmacodynamic; PK, pharmacokinetic; RMSD, root-mean-square distance

REFERENCES

- (1) Dingledine, R., Borges, K., Bowie, D., and Traynelis, S. (1999) The glutamate receptor ion channels. *Pharmacol. Rev.* 51, 7–61.
- (2) Collingridge, G. L., and Watkins, J. C. (1994) *The NMDA Receptor*, Oxford University Press, Oxford.
- (3) Kew, J. N. C., and Kemp, J. A. (2005) Ionotropic and metabotropic glutamate receptor structure and pharmacology. *Psychopharmacology* 179, 4–29.

- (4) Francotte, P., de Tullio, P., Fraikin, P., et al. (2006) In search of novel AMPA potentiators. *Recent Pat. CNS Drug Discovery* 1, 239–246.
- (5) Mayer, M. L., and Armstrong, N. (2004) Structure and function of glutamate receptor ion channels. *Annu. Rev. Physiol.* 66, 161–181.
- (6) O'Neill, M. J., Bleakman, D., Zimmerman, D. M., and Nisenbaum, E. S. (2004) AMPA receptor potentiators for the treatment of CNS disorders. *Curr. Drug Targets: CNS Neurol. Disord.* 3, 181–194.
- (7) O'Neill, M. J., and Dix, S. (2007) AMPA receptor potentiators as cognitive enhancers. *IDrugs* 10, 185–192.
- (8) Zarate, C. A., and Manji, H. K. (2008) The role of AMPA receptor modulation in the treatment of neuropsychiatric diseases. *Exp. Neurol.* 211, 7–10.
- (9) Hashimoto, K. (2009) Emerging role of glutamate in the pathophysiology of major depressive disorder. *Brain Res. Rev.* 61, 105–123.
- (10) Pirotte, B., Francotte, P., Goffin, E., et al. (2010) Ring-fused thiazidiazines as core structures for the development of potent AMPA receptor potentiators. *Curr. Med. Chem.* 17, 3575–3582.
- (11) Ward, S. E., and Harries, M. (2010) Recent advances in the discovery of selective AMPA receptor positive allosteric modulators. *Curr. Med. Chem.* 17, 3503–3513.
- (12) Pirotte, B., Francotte, P., Goffin, E., and De Tullio, P. (2013) AMPA receptor positive allosteric modulators: a patent review. *Expert Opin. Ther. Pat.* 23, 615–628.
- (13) Grove, S. J. A., Jamieson, C., Maclean, J. C. F., Morrow, J. A., and Rankovic, Z. (2010) Positive allosteric modulators of the α -amino-3-hydroxy-5-methyl-4-isoxazolepropionic acid (AMPA) receptor. *J. Med. Chem.* 53, 7271–7279.
- (14) Jin, R., Clark, S., Weeks, A. M., Dudman, J. T., Gouaux, E., and Partin, K. M. (2005) Mechanism of positive allosteric modulators acting on AMPA receptors. *J. Neurosci.* 25, 9027–9036.
- (15) Phillips, D., Sonnenberg, J., Arai, A. C., Vaswani, R., Krutzik, P. O., Kleisli, T., Kessler, M., Granger, R., Lynch, G., and Chamberline, A. R. (2002) 5'-Alkyl-benzothiadiazides: A New Subgroup of AMPA Receptor Modulators with Improved Affinity. *Bioorg. Med. Chem.* 10, 1229–1248.
- (16) Braghiroli, D., Puia, G., Cannazza, G., Tait, A., Parenti, C., Losi, G., and Baraldi, M. (2002) Synthesis of 3,4-Dihydro-2H-1,2,4-benzothiadiazine 1,1-Dioxide Derivatives as Potential Allosteric Modulators of AMPA/Kainate Receptors. *J. Med. Chem.* 45, 2355–2357.
- (17) Pirotte, B., Podona, T., Diouf, O., de Tullio, P., Lebrun, P., Dupont, L., Somers, F., Delarge, J., Morain, P., Lestage, P., Lepagnol, J., and Spedding, M. (1998) 4H-1,2,4-Pyridothiadiazine 1,1-Dioxides and 2,3-Dihydro-4H-1,2,4-pyridothiadiazine 1,1-Dioxides Chemically Related to Diazoxide and Cyclothiazide as Powerful Positive Allosteric Modulators of (R/S)-2-Amino-3-(3-hydroxy-5-methylisoxazol-4-yl)-propionic Acid Receptors: Design, Synthesis, Pharmacology, and Structure-Activity Relationships. *J. Med. Chem.* 41, 2946–2959.
- (18) Graindorge, E., Francotte, P., Boverie, S., de Tullio, P., and Pirotte, B. (2004) New Trends in the Development of Positive Allosteric Modulators of AMPA Receptors. *Curr. Med. Chem.: Cent. Nerv. Syst. Agents* 4, 95–103.
- (19) Hashimoto, K., Okamura, N., Shimizu, E., and Iyo, M. (2004) Glutamate Hypothesis of Schizophrenia and Approach for Possible Therapeutic Drugs. *Curr. Med. Chem.: Cent. Nerv. Syst. Agents* 4, 147–154.
- (20) Francotte, P., de Tullio, P., Goffin, E., Dintilhac, G., Graindorge, E., Fraikin, P., Lestage, P., Danober, L., Thomas, J.-Y., Caignard, D.-H., and Pirotte, B. (2007) Design, Synthesis, and Pharmacology of Novel 7-Substituted 3,4-Dihydro-2H-1,2,4-benzothiadiazine 1,1-Dioxides as Positive Allosteric Modulators of AMPA Receptors. *J. Med. Chem.* 50, 3153–3157.
- (21) Battisti, U. M., Jozwiak, K., Cannazza, G., Puia, G., Stocca, G., Braghiroli, D., Parenti, C., Brasili, L., Carozzo, M. M., Citti, C., and Troisi, L. (2012) 5-Arylbenthiazidiazine Type Compounds as Positive Allosteric Modulators of AMPA/Kainate Receptors. *ACS Med. Chem. Lett.* 3, 25–29.

- (22) Carrozzo, M. M., Battisti, U. M., Cannazza, G., Puia, G., Ravazzini, F., Falchicchio, A., Perrone, S., Citti, C., Jozwiak, K., Braghioroli, D., Parenti, C., and Troisi, L. (2014) Design, stereoselective synthesis, configurational stability and biological activity of 7-chloro-9-(furan-3-yl)-2,3,3a,4-tetrahydro-1H-benzo[e]pyrrolo[2,1-c][1,2,4]-thiadiazine 5,5-dioxide. *Bioorg. Med. Chem.* 22, 4667–4676.
- (23) Cannazza, G., Battisti, U. M., Carrozzo, M. M., Cazzato, A. S., Braghioroli, D., Parenti, C., and Troisi, L. (2014) Development of an in vitro liquid chromatography-mass spectrometry method to evaluate stereo and chemical stability of new drug candidates employing immobilized artificial membrane column. *J. Chromatogr. A* 1363, 216–225.
- (24) Francotte, P., Goffin, E., Fraikin, P., Lestage, P., Van Heugen, J. C., Gillotin, F., Danober, L., Thomas, J. Y., Chiap, P., Caignard, D. H., Pirotte, B., and de Tullio, P. (2010) New Fluorinated 1,2,4-Benzothiadiazine 1,1-Dioxides: Discovery of an Orally Active Cognitive Enhancer Acting through Potentiation of the 2-Amino-3-(3-hydroxy-5-methylisoxazol-4-yl)propionic Acid Receptors. *J. Med. Chem.* 53, 1700–1711.
- (25) Humphreys, W. G., and Unger, S. E. (2006) Safety Assessment of Drug Metabolites: Characterization of Chemically Stable Metabolites. *Chem. Res. Toxicol.* 19, 1564–1569.
- (26) Cannazza, G., Jozwiak, K., Parenti, C., Braghioroli, D., Carrozzo, M. M., Puia, G., Losi, G., Baraldi, M., Lindner, W., and Wainer, I. W. (2009) A novel class of allosteric modulators of AMPA/Kainate receptors. *Bioorg. Med. Chem. Lett.* 19, 1254–1257.
- (27) Cannazza, G., Carrozzo, M. M., Cazzato, A. S., Bretis, I. M., Troisi, L., Parenti, C., Braghioroli, D., Guiducci, S., and Zoli, M. (2012) Simultaneous measurement of adenosine, dopamine, acetylcholine and 5-hydroxytryptamine in cerebral mice microdialysis samples by LC-ESI-MS/MS. *J. Pharm. Biomed. Anal.* 71, 183–186.
- (28) Hill, J. R. (2003) In Vitro Drug Metabolism Using Liver Microsomes. *Current Protocols in Pharmacology*, John Wiley & Sons, Inc., Hoboken, NJ.
- (29) Battisti, U. M., Carrozzo, M. M., Cannazza, G., Puia, G., Troisi, L., Braghioroli, D., Parenti, and Jozwiak, K. (2011) Molecular modeling studies, synthesis, configurational stability and biological activity of 8-chloro-2,3,5,6-tetrahydro-3,6-dimethyl-pyrrolo[1,2,3-de]-1,2,4-benzothiadiazine 1,1-dioxide. *Bioorg. Med. Chem.* 19, 7111–7119.
- (30) Bertolino, M., Baraldi, M., Parenti, C., Braghioroli, D., Di Bella, M., Vicini, S., and Costa, E. (1993) Modulation of AMPA/kainate receptors by analogues of diazoxide and cyclothiazide in thin slices of rat hippocampus. *Receptors Channels* 1, 267–278.
- (31) Ptak, C. P., Ahmed, A. H., and Oswald, R. E. (2009) Probing the Allosteric Modulator Binding Site of GluR2 with Thiazide Derivatives. *Biochemistry* 48, 8594–8602.
- (32) Cannazza, G., Carrozzo, M. M., Battisti, U., Braghioroli, D., and Parenti, C. (2009) On-line racemization by high-performance liquid chromatography. *J. Chromatogr. A* 1216, 5655–5659.
- (33) Kumar, J., and Mayer, M. L. (2013) Functional insights from glutamate receptor ion channel structures. *Annu. Rev. Physiol.* 75, 313–337.
- (34) Isaac, J. T. R., Ashby, M. C., and McBain, C. J. (2007) The Role of the GluR2 Subunit in AMPA Receptor Function and Synaptic Plasticity. *Neuron* 54, 859–871.
- (35) Man, H.-Y. (2011) GluA2-lacking, calcium-permeable AMPA receptors - inducers of plasticity? *Curr. Opin. Neurobiol.* 21, 291–298.
- (36) Jakobsen, P., and Treppendahl, S. (1979) The structure of 1,2,4-benzothiadiazine-1,1-dioxides. *Tetrahedron* 35, 2151–2153.
- (37) Bandoli, G., and Nicolini, M. (1977) Crystal and molecular structure of diazoxide, an antihypertensive agent. *J. Cryst. Mol. Struct.* 7, 229–240.
- (38) Dupont, L. A., De Tullio, P., Boverie, S., and Pirotte, B. (2001) 3-Amino-4H-pyrrolo[2,3-e]-1,2,4-thiadiazine 1,1-dioxide. *Acta Crystallogr., Sect. E: Struct. Rep. Online* E57, o602–o603.
- (39) Novello, F. C., Bell, S. C., Abrams, E. L. A., Ziegler, C., and Sprague, J. M. (1960) Diuretics: 1,2,4-Benzothiadiazine-1,1-dioxides. *J. Org. Chem.* 25, 970–981.
- (40) Dupont, L., et al. (1995) 3-Benzamido-4H-pyrrolo[4,3-e]-1,2,4-thiadiazine 1,1-Dioxide. *Acta Crystallogr., Sect. C: Cryst. Struct. Commun.* C51, 1903–1905.
- (41) Dupont, L., Pirotte, B., De Tullio, P., and De Large, J. (1996) 3-Isopropylamino-4-methyl-4H-pyrrolo-[4,3-e][1,2,4]thiadiazine 1,1-Dioxide. *Acta Crystallogr., Sect. C: Cryst. Struct. Commun.* C52, 1741–1743.
- (42) Deeter, J., Frazier, J., Staten, G., Staszak, M., and Weigel, L. (1990) Asymmetric synthesis and absolute stereochemistry of LY248686. *Tetrahedron Lett.* 31, 7101–7104.
- (43) Randle, J. C. R., Biton, C., and Lepagnol, J. M. (1993) Allosteric potentiation by diazoxide of AMPA receptor currents and synaptic potentials. *Eur. J. Pharmacol., Mol. Pharmacol. Sect.* 247, 257–265.
- (44) Francotte, P., de Tullio, P., Goffin, E., Dintilhac, G., Graindorge, E., Fraikin, P., Lestage, P., Danober, L., Thomas, J. Y., Caignard, D. H., and Pirotte, B. (2007) Design, Synthesis, and Pharmacology of Novel 7-Substituted 3,4-Dihydro-2H-1,2,4-benzothiadiazine 1,1-Dioxides as Positive Allosteric Modulators of AMPA Receptors. *J. Med. Chem.* 50, 3153–3157.
- (45) Duthheil, F., Beaune, P., and Lorient, M.-A. (2008) Xenobiotic metabolizing enzymes in the central nervous system: Contribution of cytochrome P450 enzymes in normal and pathological human brain. *Biochimie* 90, 426–436.
- (46) Westerink, B. H. C. (2000) Analysis of biogenic amines in microdialysates of the brain. *J. Chromatogr., Biomed. Appl.* 747, 21–32.
- (47) Van der Zeyden, M., Oldenziel, W. H., Rea, K., Cremers, T. I., and Westerink, B. H. (2008) Microdialysis of GABA and glutamate: analysis, interpretation and comparison with microsensors. *Pharmacol., Biochem. Behav.* 90, 135–47.
- (48) Zielke, H. R., Zielke, C. L., and Baab, P. J. (2009) Direct measurement of oxidative metabolism in the living brain by microdialysis: a review. *J. Neurochem.* 109, 24–29.
- (49) Bourne, J. A. (2003) Intracerebral microdialysis: 30 years as a tool for the neuroscientist. *Clin. Exp. Pharmacol. Physiol.* 30, 16–24.
- (50) Pepeu, G., and Giovannini, M. G. (2004) Changes in acetylcholine extracellular levels during cognitive processes. A review. *Learn. Mem.* 11, 21–27.
- (51) Carrozzo, M. M., Cannazza, G., Pinetti, D., Di Viesti, V., Battisti, U., Braghioroli, D., Parenti, C., and Baraldi, M. (2010) Quantitative analysis of acetylcholine in rat brain microdialysates by liquid chromatography coupled with electrospray ionization tandem mass spectrometry. *J. Neurosci. Methods* 194, 87–93.
- (52) Sanacora, G., Zarate, C. A., Krystal, J. H., and Manji, H. K. (2008) Targeting the glutamatergic system to develop novel, improved therapeutics for mood disorders. *Nat. Rev. Drug Discovery* 7, 426–437.
- (53) Rosi, S., Giovannini, M. G., Lestage, P. J., Muñoz, C., Della Corte, L., and Pepeu, G. (2004) S 18986, a positive modulator of AMPA receptors with cognition-enhancing properties, increases ACh release in the hippocampus of young and aged rat. *Neurosci. Lett.* 361, 120–123.
- (54) Murase, K., Ryu, P. D., and Randic, M. (1989) Excitatory and inhibitory amino acids and peptide-induced responses in acutely isolated rat spinal dorsal horn neurons. *Neurosci. Lett.* 103, 56–63.
- (55) Paxinos, G., and Franklin, K. B. J. (2004) *The Mouse Brain in Stereotaxic Coordinates*, Gulf Professional Publishing.